Modelling of Cascaded Coplanar Waveguide Discontinuities by the Mode–Matching Approach

R. Schmidt[1], P. Russer[1,2]

[1] Technische Universität München, Lehrstuhl für Hochfrequenztechnik
Arcisstraße 21, 80290 München, Germany
[2] Ferdinand–Braun–Institut für Höchstfrequenztechnik
Rudower Chaussee 5, 12489 Berlin, Germany

Abstract

Cascaded coplanar waveguide discontinuities with transverse dimensions in the order of some micrometers are analyzed by the mode-matching approach based on a full-wave analysis of the electromagnetic field also in the metallic regions. Compared with full–wave analysis assuming perfect conductors and a subsequent loss computation based on the surface impedance model the accuracy is considerably enhanced.

Introduction

In monolithic microwave integrated circuit design coplanar waveguide (CPW) structures meet with growing interest. In recent publications the influence of the metallization thickness on the scattering characteristics of cascaded CPW discontinuities is investigated [1], [2]. The results confirm that the finite metallization thickness may significantly affect the electrical characteristics of CPW circuits. However, these approaches are based on field modelling assuming perfect conductors, which is only valid for waveguides with transverse dimensions considerably larger than the skin depth. In CPW's with strip width and metallization thickness in the skin depth's order of magnitude conductor loss influences the propagation characteristics of transmission lines [5]–[8] and hence the scattering behaviour of cascaded discontinuities. A full–wave analysis is required considering also the electromagnetic field inside the conductor. The mode matching method fulfills these requirements. However, this method has been applied up to now only to the computation of the scattering characteristics of single step discontinuities [3]. In this work the mode–matching method is extended to determine the scattering parameters of cascaded coplanar transmission line discontinuities.

Method of Analysis

Analyzing cascaded discontinuities by the mode-matching method requires the calculation of the complete set of eigenmodes in each waveguide. In Fig. 1 a coplanar waveguide (CPW) with finite metalliziation thickness inside a rectangular box with perfect electric conducting walls is depicted. Due to the symmetry with respect to the plane $x = 0$, only half of the structure has to be considered. The cross section is divided into three layers. In each of the layers l the electromagnetic field is expanded into a series of partial waves consisting of a combination of LSE_x and LSH_x longitudinal section waves, respectively. Imposing the same dependence in z-direction for each partial wave the electric and magnetic fields $\mathbf{E}^{(l)}$ and $\mathbf{H}^{(l)}$ in the layer l may be expanded in an infinite sum of LSE_x and LSH_x partial wave components:

$$\mathbf{n}_y \times \mathbf{E}^{(l)} = \sum_n \sqrt{Z_n^{(l)}} \cdot \mathbf{n}_y \times \mathbf{e}_n^{(l)}(x) \cdot \left[A_n^{(l)} e^{jk_{yn}^{(l)} y} + B_n^{(l)} e^{-jk_{yn}^{(l)} y}\right] \cdot e^{-jk_z z} \quad (1)$$

$$\mathbf{n}_y \times \mathbf{H}^{(l)} = \sum_n \sqrt{Y_n^{(l)}} \cdot \mathbf{n}_y \times \mathbf{h}_n^{(l)}(x) \cdot \left[A_n^{(l)} e^{jk_{yn}^{(l)} y} - B_n^{(l)} e^{-jk_{yn}^{(l)} y}\right] \cdot e^{-jk_z z} \quad (2)$$

where $\mathbf{e}_n^{(l)}$ and $\mathbf{h}_n^{(l)}$ are the vector–valued expansion functions for the electric and magnetic field respectively. $\mathbf{n}_y$ is the unit vector in y–direction. The field expansions in two neighbouring layers l and k are matched by applying the method of moments to the tangential field continuity conditions $\mathbf{n}_y \times (\mathbf{E}^{(l)} - \mathbf{E}^{(k)}) = 0$ and $\mathbf{n}_y \times (\mathbf{H}^{(l)} - \mathbf{H}^{(k)}) = 0$ at their horizontal boundary. Hence we define the inner product

$$\langle \mathbf{u}, \mathbf{v} \rangle = \int_0^a \mathbf{u}^* \cdot \mathbf{v} \, dx \quad (3)$$

TU 4D

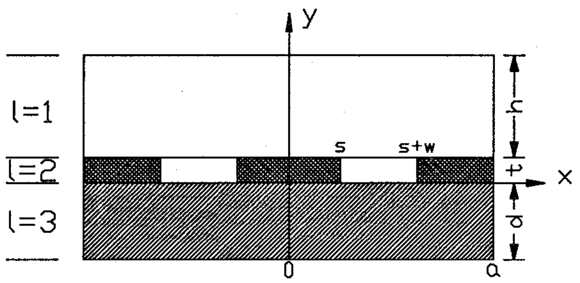

Figure 1: Coplanar waveguide cross section

Defining $\tilde{\mathbf{e}}_n^{(l)}$ and $\tilde{\mathbf{h}}_n^{(l)}$ as the expansions functions of the electromagnetic field which propagates in the $-z$ direction with $e^{jk_z z}$ the following orthogonality relations hold:

$$\langle \tilde{\mathbf{e}}_m^{(l)*}, \mathbf{n}_y \times \mathbf{h}_n^{(l)} \rangle = \delta_{mn} \quad (4)$$
$$\langle \mathbf{e}_m^{(l)*}, \mathbf{n}_y \times \tilde{\mathbf{h}}_n^{(l)} \rangle = \delta_{mn} \quad (5)$$

Hence the coupling between the partial wave coefficients $A_n^{(l)}$, $A_n^{(k)}$ and $B_n^{(l)}$, $B_n^{(k)}$ can be described by a symmetric generalized scattering matrix (GSM) provided the set of normalized partial waves is complete. In the computation the field expansion must be truncated to a finite number of partial waves. In order to preserve the symmetry of the GSM we use the complex conjugate magnetic field expansion functions $\tilde{\mathbf{h}}_n^{(l)*}$ as electric field test functions and the complex conjugate electric field expansion functions $\tilde{\mathbf{e}}_n^{(k)*}$ and as magnetic field test functions or vice versa. These two possible sets of test functions lead to the following two different linear systems of equations

$$\text{A:} \quad \langle \tilde{\mathbf{h}}_m^{(l)*}, \mathbf{n}_y \times (\mathbf{E}^{(l)} - \mathbf{E}^{(k)}) \rangle = 0$$
$$\langle \tilde{\mathbf{e}}_m^{(k)*}, \mathbf{n}_y \times (\mathbf{H}^{(l)} - \mathbf{H}^{(k)}) \rangle = 0$$

$$\text{B:} \quad \langle \tilde{\mathbf{h}}_m^{(k)*}, \mathbf{n}_y \times (\mathbf{E}^{(l)} - \mathbf{E}^{(k)}) \rangle = 0$$
$$\langle \tilde{\mathbf{e}}_m^{(l)*}, \mathbf{n}_y \times (\mathbf{H}^{(l)} - \mathbf{H}^{(k)}) \rangle = 0$$

Substituting (1) and (2) into these two sets of equations it can be shown that modelling the boundary between the layers l and k by equivalent surface currents $\mathbf{J}_A^{(lk)}$ and $\mathbf{M}_A^{(lk)}$ [11] leads to the same set of equations, if correspondingly to the above set partition the currents are related to the fields by

$$\text{A:} \quad \mathbf{J}_A^{(lk)} = \mathbf{n}_y \times \mathbf{H}^{(l)} \quad \text{and} \quad \mathbf{M}_A^{(lk)} = \mathbf{E}^{(k)} \times \mathbf{n}_y$$
$$\text{B:} \quad \mathbf{J}_A^{(lk)} = \mathbf{n}_y \times \mathbf{H}^{(k)} \quad \text{and} \quad \mathbf{M}_A^{(lk)} = \mathbf{E}^{(l)} \times \mathbf{n}_y$$

Requesting fast convergence the test functions of set 'B' are to be preferred in the field matching procedures between the layers $l = 2$ and $k = 3$, because according to the above stated correspondence the very small magnetic current on the surface of the metallization layer can be faster approximated by this set. Accordingly the field matching between the layers $l = 1$ and $k = 2$ is performed using the test functions of set 'A'.
By combining all continuity equations and boundary conditions at the horizontal waveguide walls at $y = -d$ and $y = t+h$ sufficient relationships are obtained to determine the complex propagation constants k_z and the unknown partial wave amplitudes of the fundamental and higher-order modes. In the next step these eigenmodes are matched at each waveguide discontinuity by imposing the field continuity over the whole waveguide cross section. The coupling of the incident and reflected eigenmodes on both sides of the discontinuity can be described by a GSM. The scattering parameters are

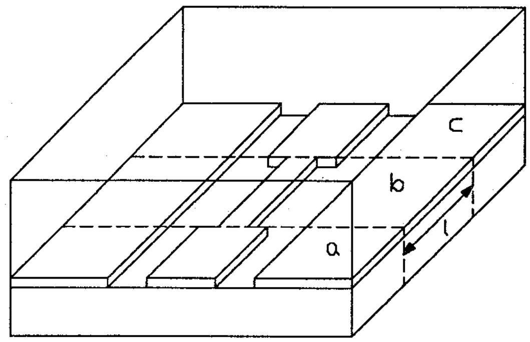

Figure 2: Cascaded coplanar waveguide discontinuities

again determined by applying the method of moments to the field continuity conditions. The inner product of two vectors is now defined as the integral of the scalar product of these two vectors over the entire waveguide cross section. Correspondingly to the one–dimenional matching between two layers the test functions in this two-dimensional case are analogously chosen to ensure the symmetry of the GSM of the waveguide discontinuity. Matching the eigemode expansion of waveguide a and b in Fig. 2 we thus use the complex conjugate magnetic field expansion functions of waveguide b as electric test functions and the complex conjugate electric field expansion functions of waveguide a as magnetic test functions.
In the last step the scattering characteristics of cascaded waveguide discontinuities are calculated by combining successively the GSM's of the waveguide step discontinuities and of the waveguide transmissions lines between the junctions [12]. By using this approach higher–order mode interactions between junctions are included.

Numerical Results

First we calculated the propagation characteristics of a CPW with a metallization thickness which is not large in comparison with the skin depth. The CPW was measured by R.B. Marks from the NIST. The experimental data are taken from [7]. In Fig. 3 and 4 the frequency dependence of the propagation and attenuation constant is plotted and compared with the results of a full-wave field analysis assuming perfect conductors. In this case conductor loss is computed by modelling the field inside the conductor by a surface impedance and a surface impedance matrix description. In the surface impedance matrix description the coupling of the fields on top and bottom of the metallization layer is taken into account. In Fig. (3) $\epsilon_{r,eff}$ exhibits a negative slope over the whole frequency band. This behaviour can only be modelled by field analysis taking into account also the metallic losses.

We calculated the reflection coefficient of cascaded CPW step discontinuities using the same parameters as Alessandri et al [1], who considered the metallization layer a perfect conductor and verified their results by experiments. The results of both calculations are shown in Fig. 5. As can be seen, the results agree excellently, thus confirming the validity of the mode–matching approach described above.

Fig. 6 shows the dependence of the fundamental mode scattering parameters of cascaded CPW discontinuites on the distance L between the discontinuities for perfect and non–perfect conductors. The attenuation of the fundamental eigenmode of the inner waveguide b with an perfect metallization layer is hereby approximated by the two surface impedance models. The periodic variation of the scattering parameter $S11$ in Fig. 6 indicates the existence of a standing wave between the two cascaded discontinuities [2]. Fig. 6 shows that the resonant behaviour in a CPW with transverse dimensions, which are not large compared to the skin depth, can be correctly modelled only by a self-consistent description of the metallic losses.

In Fig. 7 the transmission coefficient of a low–pass filter of 11th order is plotted over the frequency band. Assuming perfect conductors the filtering behaviour deviates strongly from the results obtained by a self–consistent compution of the metallic losses.

Conclusion

A full–wave analysis has been performed to calculate the scattering characteristics of cascaded coplanar waveguide discontinuities. It was found that the transmission and reflection coefficients are strongly affected by metallic losses if the line geometries of the waveguide structure are in the order of the skin depth.

Acknowledgement

This work has been supported by the Siemens AG, Munich.

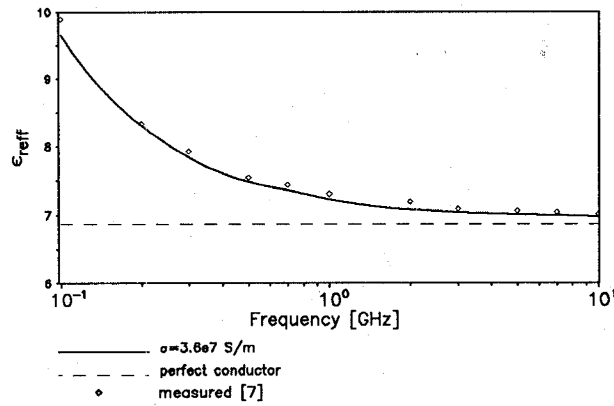

Figure 3: Effectiv dielectric constant (s=9.9 μm, w=5.1μm. Subtrate: ϵ_r=12.9, $\tan\delta = 1 \cdot 10^{-4}$, thickness=1 mm. f=10 GHz)

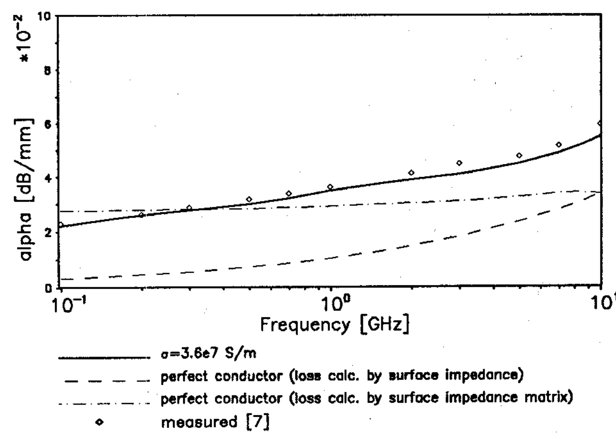

Figure 4: Attentuation (s=9.9 μm, w=5.1μm. Subtrate: ϵ_r=12.9, $\tan\delta = 1 \cdot 10^{-4}$, thickness=1 mm. f=10 GHz)

References

[1] F. Alessandri, G. Baini, M. Mongiardo, R. Sorrentino, "A 3-D Mode Matching Technique for the Efficient Analysis of Coplanar MMIC Discontinuities with Finite Metallization Thickness", *IEEE Trans. Microwave Theory Tech.*, vol. MTT-41, pp. 1625-1629, September 1993

[2] T.W. Huang, T. Itoh, "The Influence of Metallization Thickness on the Characteristics of Cascaded Junction Discontinuities of Shielded Coplanar Type Transmission Line", *IEEE Trans. Microwave Theory Tech.*, vol. MTT-41, pp. 693-697, April 1993

[3] R. Schmidt, P. Russer, "Full–Wave Analysis of Coplanar Waveguide Discontinuities by Partial Wave Synthesis", *10th Anniversary ACES Conference*, Monterey, 1994, pp. 576-583

[4] Q. Xu, K.J. Webb, R. Mittra, "Study of Modal Solution Procedures for Microstrip Step Discontinuities", *IEEE Trans. Microwave Theory Tech.*, vol. MTT-37, pp. 381-386, February 1989

[5] K. Wu, R. Vahldieck, J.L. Fikart, H. Minkus, "The Influence of Finite Conductor Thickness and Conductivity on Fundamental and Higher-Order Modes in Miniature Hybrid MIC's (MHMIC's) and MMIC's", *IEEE Trans. Microwave Theory Tech.*, vol. MTT-41, pp. 421-430, March 1993

[6] W. Heinrich, "Full–Wave Analysis of Conductor Losses on MMIC Transmission Lines", *IEEE Trans. Microwave Theory Tech.*, vol. MTT-38, pp. 1468-1472, October 1990

[7] W. Heinrich, "Beiträge zur Simulation monolithisch integrierter Höchstfrequenzschaltungen", Fortschrittsberichte VDI, Reihe 21: Elektrotechnik, Nr. 136, 1993

[8] Y.C. Shih, M. Maher, "Characterization of conductor–backed coplanar waveguides using accurate on-wafer measurement techniques", in 1990 IEEE MTT-S Int. Microwave Symp. Dig., Dallas, pp. 1129-1132

[9] J. Kessler, R. Dill, P. Russer, "Field Theory Investigation of High–T_c Superconducting Coplanar Waveguide Transmission Lines and Resonators", *IEEE Trans. Microwave Theory Tech.*, vol. MTT-39, pp. 1566-1574, September 1991

[10] T.S. Chu, T. Itoh, "Generalized Scattering Matrix Method for Analysis of Cascaded and Offset Microstrip Step Discontinuities", *IEEE Trans. Microwave Theory Tech.*, vol. MTT-34, pp. 280-284, February 1986

[11] D.N. Zuckermann, P. Diament, "Rank Reduction of Ill–Conditioned Matrices in Waveguide Junction Problems", *IEEE Trans. Microwave Theory Tech.*, vol. MTT-25, pp. 613-619, July 1977

[12] T.S. Chu, T. Itoh, "Generalized Scattering Matrix Method for Analysis of Cascaded and Offset Microstrip Step Discontinuities", *IEEE Trans. Microwave Theory Tech.*, vol. MTT-34, pp. 280-284, February 1986

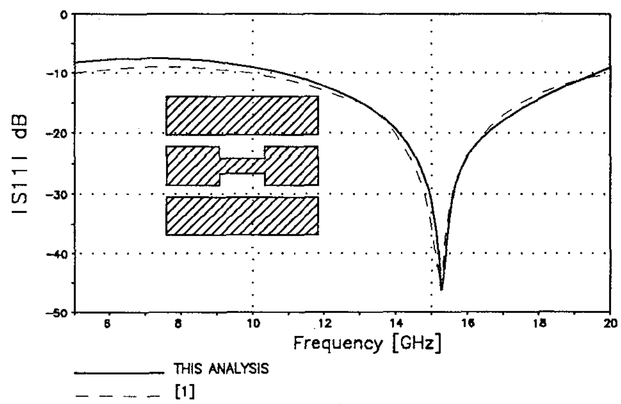

Figure 5: Comparison of computed return loss of double step discontinuity in CPW. (Feeding line: width 0.5 mm, gap 0.2 mm. Central line width: 0.2 mm. Distance between steps: L=4.36 mm. Substrate: ϵ_r=9.9, thickness 0.635 mm. Metallization thickness 35 μm. Housing: WR28)

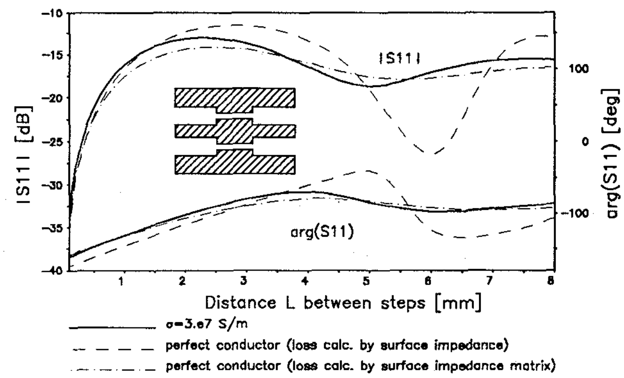

Figure 6: S11 of cascaded CPW discontinuity (s^a=6.9 μm, w^a=10.1μm, s^b=9.9 μm, w^b=5.1μm, s^c=6.9 μm, w^c=10.1μm, Subtrate: ϵ_r=12.9, thickness=1 mm, $\tan\delta = 1 \cdot 10^{-4}$. metallization thickness t=0.2μm. f=10 GHz)

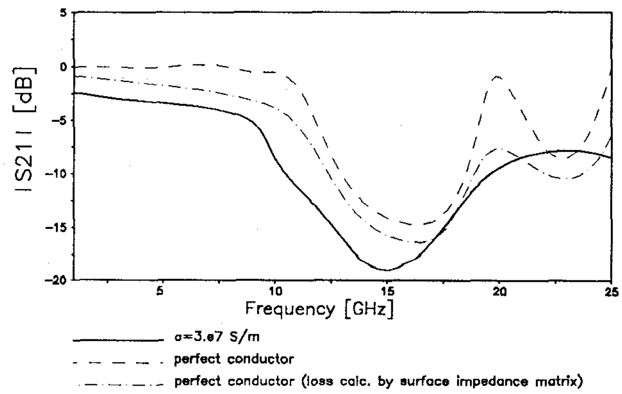

Figure 7: $|S21|$ of low–pass filter of 11th order (Subtrate: ϵ_r=12.9, thickness=500μm, $\tan\delta = 1 \cdot 10^{-4}$. metallization thickness t=1.0μm)